JACS
JOURNAL OF THE AMERICAN CHEMICAL SOCIETY

Article

pubs.acs.org/JACS

CO_2 Stimuli-Responsive, Injectable Block Copolymer Hydrogels Cross-Linked by Discrete Organoplatinum(II) Metallacycles via Stepwise Post-Assembly Polymerization

Wei Zheng,[†] Guang Yang,[‡] Nannan Shao,[∥] Li-Jun Chen,[†] Bo Ou,[†] Shu-Ting Jiang,[†] Guosong Chen,*[,‡] and Hai-Bo Yang*[,†]

[†]Shanghai Key Laboratory of Green Chemistry and Chemical Processes, School of Chemistry and Molecular Engineering, East China Normal University, Shanghai 200062, P. R. China

[‡]The State Key Laboratory of Molecular Engineering of Polymers and Department of Macromolecular Science, Fudan University, Shanghai 200433, P. R. China

[∥]State Key Laboratory of Polymer Physics and Chemistry, Changchun Institute of Applied Chemistry, Chinese Academy of Science Changchun 130022, P. R. China

Supporting Information

ABSTRACT: Supramolecular polymeric gels cross-linked by well-defined, discrete metal−organic macrocycles (MOMs) or metal−organic cages have become a prevailing topic within the field of supramolecular self-assembly. However, the realization of supramolecular polymeric hydrogels cross-linked by discrete organometallic architectures with good biocompatibility is still a great challenge. Herein, we present the successful preparation of CO_2 stimuli-responsive, injectable block copolymer hydrogels cross-linked by discrete organoplatinum(II) metallacycles. Through the combination of coordination-driven self-assembly and *stepwise* post-assembly polymerization, star block copolymers (SBCPs) containing well-defined hexagonal metallacycles as cores were successfully prepared, which featured CO_2 stimuli-responsive properties including CO_2-triggered morphology transition and CO_2-induced thermoresponsive behavior. Interestingly, the resultant SBCPs were capable of forming supramolecular hydrogels with MOMs as junctions near physiological temperature, which allowed the realization of a reversible gel-to-sol transformation through the removal and addition of CO_2. More importantly, the resultant supramolecular hydrogels presented good cytocompatibility in vitro. Therefore, this study provides a new strategy for the construction of new "smart" supramolecular hydrogels with promising applications as biological materials.

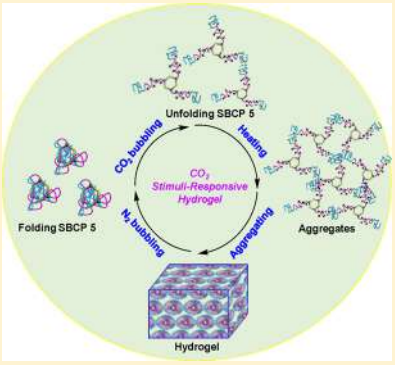

INTRODUCTION

Supramolecular gels, as a family of classical soft matter, have evolved to be one of the most attractive topics within supramolecular chemistry and materials science due to their wide applications in tissue engineering, drug and protein delivery, actuators and sensors, etc.[1] Very recently, supramolecular polymeric gels cross-linked by well-defined, discrete metal−organic macrocycles (MOMs)[2] or metal−organic cages (MOCs)[3] have received much attention. The combination of relatively rigid, discrete metal−organic scaffolds with elastic polymer networks allows for the construction of a new class of hybrid soft materials with tunable viscoelastic properties as well as multiple functions arising originally from metallosupramolecular architectures. For example, in 2013, Stang and co-workers constructed a new family of supramolecular polymers containing well-defined rhomboidal or hexagonal MOMs via hierarchical coordination-driven self-assembly and hydrogen-bonding interfaces, some of which were capable of forming gel-like soft matter through the addition of dichloromethane.[2a] Subsequently, we reported cross-linked polymer organogels with multiple stimuli-responsive behaviors from discrete multipillar[5]arene MOMs driven by hierarchical self-assembly.[2b] In 2015, Johnson and co-workers prepared a new highly branched and loop-rich gel in DMSO through formation of MOCs linked by polymers.[3a] Very recently, the same group successfully realized thermally responsive supramolecular copolymer organogels cross- linked by M_xL_y-type MOCs in 2-ethylhexanol as the solvent.[3b]

However, although great achievements have been made in this field, most known supramolecular polymeric gels cross-linked by discrete organometallic architectures[2,3] are generated in organic solvents. In general, good biological materials feature the characteristics of facile preparation, tissue adhesion, excellent biocompatibility, robust mechanical properties, and bioactivity. However, the majority of supramolecular coordination complexes display poor solubility in water and sometimes suffer from being potentially cytotoxic, thus limiting their applications as real biomaterials. With the goal of applying these supramolecular gels as biomaterials and further making them

Received: July 13, 2017
Published: September 8, 2017

DOI: 10.1021/jacs.7b07303
J. Am. Chem. Soc. 2017, 139, 13811−13820

Scheme 1. Graphical Representation of the Construction of Organoplatinum(II) Metallacycle and Star Supramolecular Block Copolymers

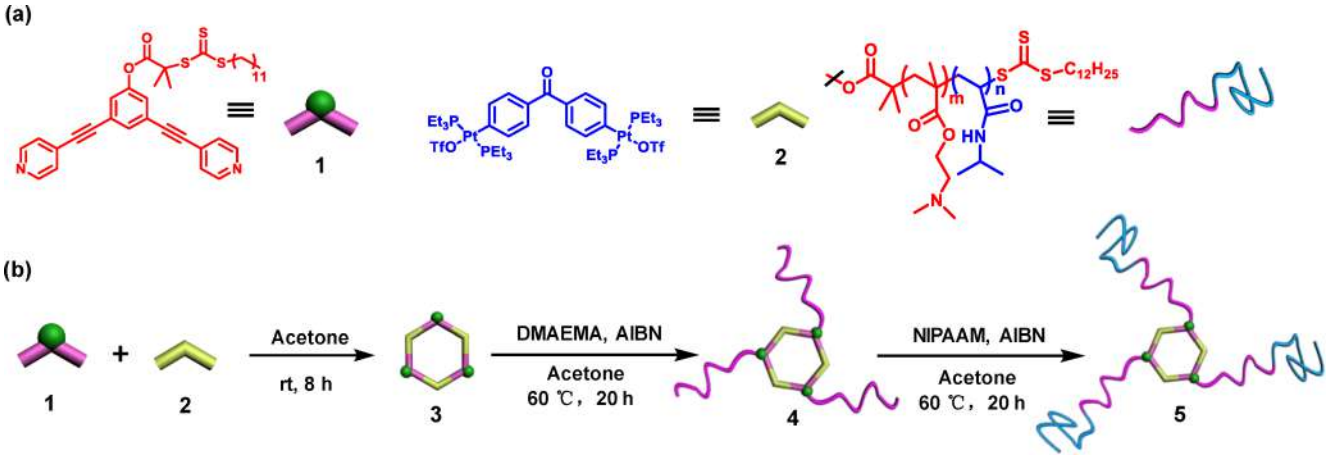

adaptive to physiological environments, the design and construction of new supramolecular polymeric hydrogels cross-linked by well-defined, discrete MOMs or MOCs, especially those with stimuli-responsiveness as well as good biocompatibility, are indeed desired. In 2015, Johnson and co-workers reported a new family of supramolecular hydrogels cross-linked by M_4L_4 square junctions through self-assembly of PEG decorated ligands with Fe^{2+} or Ni^{2+}, which was successfully employed to realize the photoinduced drug release.[3c] In the same year, Nitschke and co-workers reported a new family of polymer hydrogels that were cross-linked through their own subcomponent self-assembled MOCs.[3d] They revealed that benzene and furan could be encapsulated and released from the cages in these soft materials. Very recently, we demonstrated that the combination of a thermoresponsive polymer with discrete, well-defined MOMs through post-assembly polymerization allowed the generation of supramolecular polymeric hydrogels with self-healing properties.[2c]

It should be noted that the post-assembly modification[4] strategy provides an opportunity to fine-tune the structures and properties of supramolecular architectures, thus leading to construction of higher order complexity with additional functionality after the initial self-assembly. Considering that the relatively rigid MOMs or MOCs often offer very well-defined scaffolds for the precise positioning of functional groups and good control over the exact number of functional moieties per assembly, we envisioned that stepwise post-assembly polymerization might allow for the preparation of new polymeric hydrogels cross-linked by well-defined, discrete MOMs or MOCs with potential as biomaterials, which has been rarely explored in this field.

Herein, we present the successful combination of coordination-driven self-assembly[5,6] and *stepwise* post-assembly polymerization to prepare a new family of star block copolymers (SBCPs) containing well-defined MOMs as cores. The obtained star block copolymers featured carbon dioxide (CO_2) stimuli-responsive behavior including CO_2-triggered morphology transition, CO_2-induced thermoresponsive behavior, and even CO_2-promoted hydrogel formation. For instance, a new family of supramolecular polymeric hydrogels with MOMs as junctions were easily obtained upon heating an aqueous SBCP solution after it was treated with CO_2 to 34 °C at a concentration as low as 2.5 wt %. Consequently, upon bubbling N_2 into the obtained hydrogels, a reverse gel-to-sol transition was also realized. It should be noted that as a benign, abundant, and nontoxic trigger, CO_2 has been extensively explored to prepare stimuli-responsive functional materials in recent years.[7] For instance, CO_2-responsive polymers have found potential applications in diverse fields such as CO_2 capture and monitoring, separation, encapsulation, and CO_2-switchable vesicles.[8] In particular, since CO_2 is a key metabolite in cells, with good biocompatibility and biomembrane permeability,[9] it has proven to be an excellent stimulus to trigger physiological environment changes. However, compared to numerous examples of hydrogels responsive to other stimuli such as temperature, pH, and light, CO_2 stimuli-responsive hydrogels have been relatively less explored.[10] To the best of our knowledge, this study presents the first example of CO_2-switchable, injectable, block copolymer hydrogel cross-linked by well-defined, discrete MOMs, which also feature good cytocompatibility.

RESULTS AND DISCUSSION

Construction of SBCPs Containing Hexagonal MOMs via Stepwise Post-Assembly Polymerization. With the aim of preparing functionalized SBCPs containing well-defined, discrete MOMs as cores, *N*-isopropylacrylamide (NIPAAM) was selected as a thermoresponsive monomer since poly(*N*-isopropylacrylamide) (PNIPAAM) features typical LCST (lower critical solution temperature) behavior near human body temperature.[11] Moreover, in this study, *N,N*-dimethylaminoethyl methacrylate (DMAEMA) was explored as another block due to the CO_2-responsiveness and low cytotoxity of poly(*N,N*-dimethylaminoethyl methacrylate) (PDMAEMA).[12]

Based on the general principles of coordination-driven self-assembly,[5] combining three 120° donor building blocks with three 120° acceptor linkers can result in the formation of a discrete hexagonal metallacycle.[13] Thus, as shown in Scheme 1, 120° dipyridyl building block **1** substituted with trithioester, a typical chain-transfer agent (CTA) for reversible addition−fragmentation chain-transfer (RAFT) polymerization,[14] was designed and synthesized. Then, coordination-driven self-assembly of **1** with 120° di-Pt(II) acceptor **2** in acetone-d_6 provided a discrete hexagonal metallacycle **3** decorated with three CTA moieties at alternating vertexes. The structure of tris-CTA hexagon **3** was well characterized through both

DOI: 10.1021/jacs.7b07303
J. Am. Chem. Soc. 2017, 139, 13811−13820

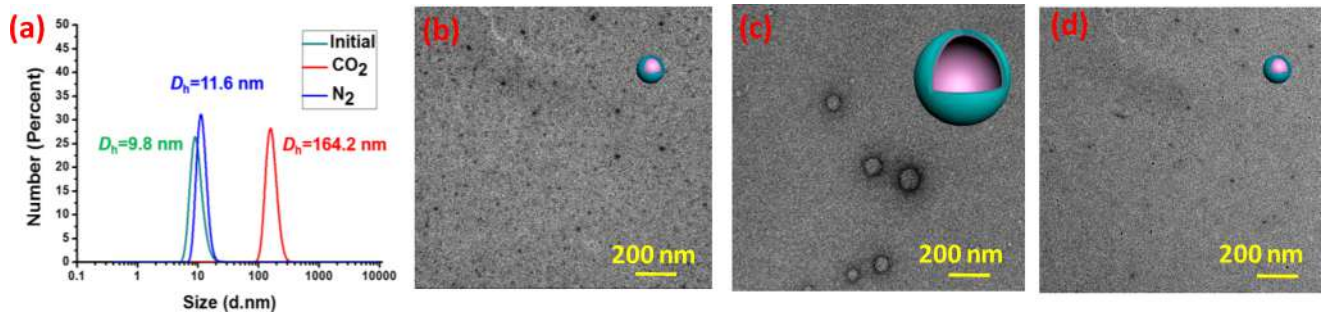

Figure 1. (a) DLS data for the size change of SBCP **5** in aqueous solution (1.0 mg/mL); no stimulus (green line), 1 min of CO_2 (red line), and subsequent 10 min of N_2 (blue line). TEM images of SBCP **5** in aqueous solution (1.0 mg/mL), (b) no stimulus, (c) 1 min of CO_2, and (d) subsequent 10 min of N_2.

multinuclear NMR (^{1}H and ^{31}P) and ESI-TOF-MS spectrometry (Figure S38).[2c] With the tris-CTA hexagonal metallacycle **3** in hand, the subsequent *stepwise* post-assembly polymerization was performed to prepare star block copolymers possessing well-defined, discrete MOMs as the main scaffold (Scheme 1). The intermediate star supramolecular polymer **4** was prepared by polymerizing DMAEMA in the presence of the corresponding tris-CTA metallacycle **3** and azodiisobutyronitrile (AIBN) as an initiator with a molar ratio of [DMAEMA]/[tris-CTA metallacycle]/[AIBN] = 600:1:0.5 in acetone. The tube was sealed under vacuum after the mixture was degassed by three freeze−evacuate−thaw circles, and the subsequent polymerization was performed at 60 °C for 20 h. Polymer **4** was isolated by precipitation in cold *n*-hexane and then dried under vacuum at room temperature overnight to afford a yellow powder. Subsequently, the targeted SBCP **5** was finally obtained from the intermediate star polymer **4** by polymerizing NIPAAM through a similar procedure.

The structures of both the intermediate star polymer **4** and SBCP **5** were well characterized by using FTIR, multinuclear (^{1}H and ^{31}P) NMR spectroscopy, and gel permeation chromatography (GPC), which provided strong support for the formation of star-shaped supramolecular block copolymers containing a well-defined hexagon as their core. For instance, the FTIR spectrum of SBCP **5** displayed the typical absorption bands of PDMAEMA ($\nu_{C=O}$ = 1721 cm^{-1} and ν_{C-N} = 1146 cm^{-1}) as well as PNIPAAM ($\nu_{C=O}$ = 1639 cm^{-1} and ν_{C-C} = 2971 cm^{-1}), which is consistent with the formation of poly(DMAEMA-*co*-NIPAAM) species (Figure S33). In addition, in the ^{1}H NMR spectrum (Figure S1) of SBCP **5**, the characteristic signals of PDMAEMA, such as δ = 2.53 ppm and δ = 4.07 ppm attributed to methyl protons (end-up group) and methylene protons, respectively, were clearly observed. Moreover, signals at δ = 4.0 ppm and δ = 1.1 ppm attributed to the methine protons and methyl protons of isopropyl groups in PNIPAAM, respectively, as well as the signal at δ = 6.80−7.45 ppm ascribed to the NH of amide groups, *etc.*, were found. Together, the listed characterization agreed well with the generation of a star-shaped block copolymer. It should be noted that compared to the parent tris-CTA metallacycle **3**, the signals corresponding to pyridyl moieties in the ^{1}H NMR spectra of both the intermediate star polymer **4** and the star block copolymer **5** remained almost unchanged (Figure S1). Similarly, the ^{31}P {^{1}H} NMR spectra of polymers **4** and **5** (Figure S1) exhibited a singlet at 14.43 or 14.41 ppm, respectively, which was almost the same as that of the original tris-CTA metallacycle (14.50 ppm). These findings indicated that the controlled *stepwise* post-assembly RAFT polymerization allowed for the formation of a new star-shaped block copolymer with the well-defined metallacycle as the core.

Furthermore, the molecular weights of polymers **4** and **5** were determined to be $M_{n,GPC}$ = 42.1 kDa and $M_{n,GPC}$ = 76.3 kDa, respectively, with a relatively narrow molecular distribution (for polymer **4**, PDI = 1.23; for polymer **5**, PDI = 1.30), based on GPC analysis (Figure S2). In addition, the degree of polymerization of PDMAEMA or PNIPAAM in each arm was determined to be 105 and 123, respectively, through NMR characterization, which was thus denoted as MOM-(PDMAEMA$_{105}$-*b*-PNIPAAM$_{123}$)$_3$. To obtain further structural information, dynamic light scattering (DLS) and transmission electron microscopy (TEM) were employed to investigate the morphology of SBCP **5** in aqueous solution. As displayed in Figure 1a, for the aqueous solution of SBCP **5** with a concentration of 1.0 mg/mL, the average hydrodynamic diameter (D_h) was determined to be approximately 9.8 nm through investigation by DLS. In addition, TEM study of SBCP **5** revealed spherical micelles with an average diameter of ∼10 nm (Figure 1b and Figure S6), which was close to the hydrodynamic diameter determined by DLS. Notably, with the increase in concentration of SBCP **5** from 1.0 mg/mL to 10.0 mg/mL, the resultant size determined by DLS was almost the same (Figure S9), which indicated that SBCP **5** was stabilized individually as unimolecular micelles. It is reported that in some cases of core−shell-type polymers, a sufficiently high molecular weight as well as a high number of linear arms allow for the formation of unimolecular micelles, thus stabilizing the individual polymer without any further self-assembly.[15] In this study, the relatively hydrophobic metallacycle was probably wrapped by three self-folded block copolymer arms, thus leading to the generation of unimolecular micelles in aqueous solution.

CO_2 Stimuli-Responsive Behavior of Star Block Copolymer 5. PDMAEMA has been explored as a weak polybase to react with CO_2 to construct CO_2-responsive materials.[12] The presence of PDMAEMA thus prompted us to investigate the CO_2-responsive behavior of SBCP **5** by using DLS and TEM. Very interestingly, upon passing CO_2 through the aqueous solution of SBCP **5** (1.0 mg/mL), the average value of D_h was found to increase to 164.2 nm as determined by DLS (Figure 1a). More importantly, this CO_2-stimulated morphology transformation was reversible. After bubbling N_2 for 10 min at room temperature into the solution previously treated with CO_2, the D_h value decreased from 164.2 nm back to 11.6 nm. Several successive morphology transition cycles were successfully realized as evidenced by DLS (Figure S10). Further TEM investigation revealed that large vesicles with an

DOI: 10.1021/jacs.7b07303
J. Am. Chem. Soc. 2017, 139, 13811−13820

Scheme 2. Schematic of CO_2-Triggered Morphology Transition of Star Block Copolymer 5 in Water

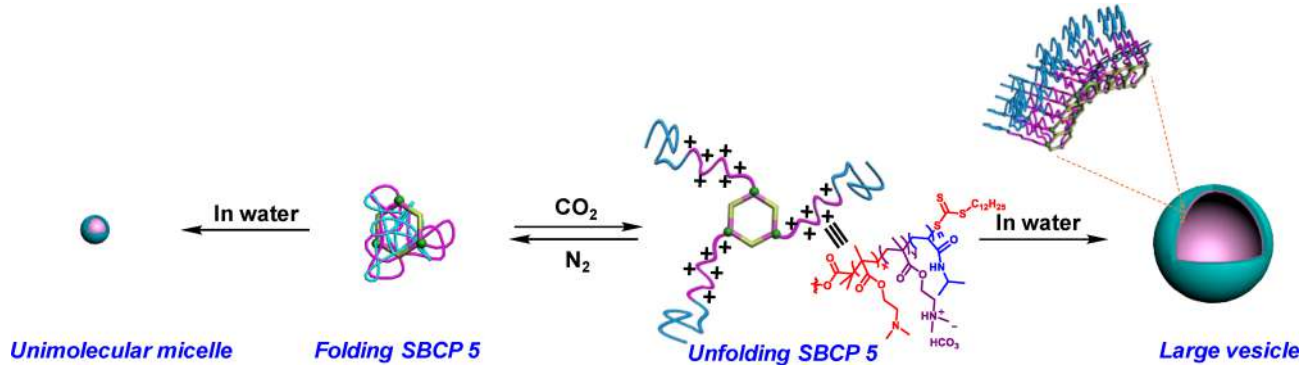

average diameter of ~120 nm were formed after CO_2 was bubbled into the aqueous solution of SBCP **5** (Figure 1c and Figure S7). This result clearly reveals a sharp morphology transition from unimolecular micelles into large vesicles trigged by CO_2. In addition, after N_2 was bubbled into the vesicle solution, the expanded vesicles were found to shrink into the small micelles, as evidenced by TEM (Figure 1d and Figure S8). Additionally, ^{1}H NMR was performed to further understand this CO_2-triggered morphology transition of SBCP **5** in aqueous solution. The change of the ^{1}H NMR spectra of SBCP **5** in D_2O with the addition and removal of CO_2 was recorded as displayed in Figure S11. After inletting CO_2 into the solution of SBCP **5** in D_2O for 1 min to protonate the PDMAEMA block, resonance peaks f, g, and h of PDMAEMA at 2.0−3.0 and 4.1 ppm distinctly shifted to lower field. Further CO_2 injection for another 5 min resulted in a clear shift of the characteristic peaks of PDMAEMA to the lower field. Subsequently, after removal of CO_2 with N_2, the chemical shifts of peaks f, g, and h returned to the original position. Notably, the typical peaks of PNIPAAM such as peaks k and i were almost unchanged with the addition and removal of CO_2, demonstrating that the reaction of CO_2 with PDMAEMA rather than PNIPAAM was the key driving force for the observed morphology transformation.

Combining all the above results, we proposed a possible explanation for such CO_2-triggered micelle−vesicle transition. Before being treated with CO_2, SBCP **5** formed stable unimolecular micelles in aqueous solution, in which the hydrophobic metallacycle was probably wrapped by the folding block copolymer chains. Upon bubbling CO_2 into the aqueous solution of SBCP **5**, the tertiary amine of PDMAEMA was protonated by carbonic acid, thus leading to the formation of the charged and water-soluble ammonium bicarbonates. Then, an unfolding star-shaped block copolymer containing the hydrophobic metallacycle as the core surrounded by hydrophilic block copolymers was obtained as a result of the repulsive interactions caused by the existence of multiple positive charges within the protonated PDMAEMA chains (Scheme 2), thus allowing for the existence a typical supramolecular amphiphilic species.[16] Driven by the hydrophilic/hydrophobic interactions, this supramolecular amphiphilic species subsequently aggregated into large vesicles in aqueous solution, which was consistent with the self-assembly behavior of a typical previously reported supramolecular amphiphilic structure.[2d] With the removal of CO_2 with N_2, the protonation of dimethylamino groups in PDMAEMA was weakened, leading to the clear hydrophilicity decrease of PDMAEMA segments. Thus, the vesicles converted into the unimolecular micelles.

Since PNIPAAM has also been explored as a smart polymer that usually exhibits LCST behavior, the thermoresponsive behavior of the obtained star block copolymer **5** was then investigated. Upon heating to 31 °C, the clear aqueous solution of SBCP **5** (3.0 mg/mL) turned into a white opaque suspension, which then regained transparency after cooling to room temperature (Figure S15). A temperature-controlled UV/vis spectrometer was used to measure the clouding point (T_{cloud}) of SBCP **5** by investigating the change in transmittance at 500 nm. As shown in Figure 2a, the transmittance curve displayed the transition with changing temperature, and the final T_{cloud} was determined to be 31 °C for SBCP **5**. Impressively, further investigation revealed that SBCP **5** displayed CO_2-induced thermoresponsive behavior. After CO_2 was bubbled into the aqueous solution of SBCP **5** for 1 min, T_{cloud} increased to 33 °C. Subsequently, after N_2 was passed

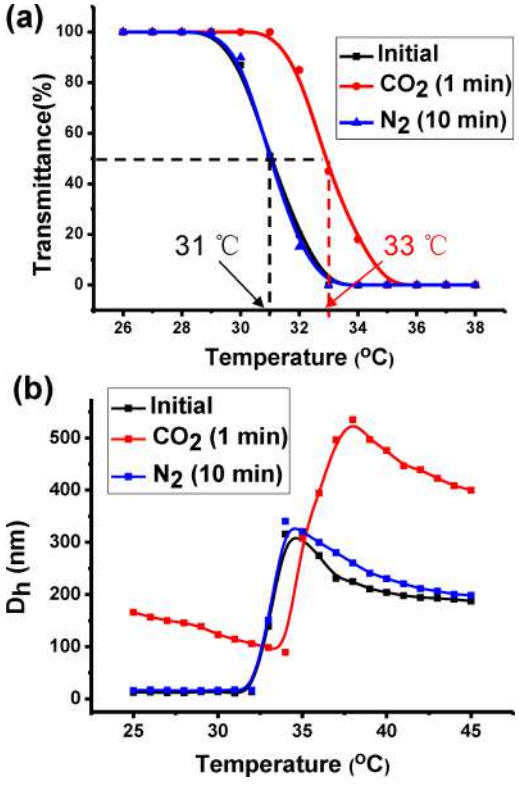

Figure 2. (a) Transmittance curves and (b) temperature dependence of hydrodynamic diameter (D_h) of SBCP **5** in aqueous solution under different conditions (3.0 mg/mL).

DOI: 10.1021/jacs.7b07303
J. Am. Chem. Soc. 2017, 139, 13811−13820

through the solution for 10 min, T_{cloud} recovered to its initial value.

To obtain further insight into such CO_2-induced thermoresponsive behavior, variable-temperature (VT) DLS was performed. Figure 2b shows the plots of the hydrodynamic diameter (D_h) of SBCP **5** in aqueous solution (3.0 mg/mL) at different temperatures with and without the existence of CO_2 as a stimulus. It was found that before treatment with CO_2, the D_h values of SBCP **5** were approximately 10 nm and changed slightly at low temperatures from 25 to 32 °C. However, when the solution temperature increased from 32 to 35 °C, the D_h sharply increased from 10 to 300 nm. The critical temperature was found to be 32 °C, which was close to the T_{cloud} obtained from the UV measurements. We rationalized that the increase in temperature weakened the hydrogen bonds between PNIPAAM and water molecules and made SBCP **5** more hydrophobic.[17] Therefore, the increased hydrophilic/hydrophobic interactions between supramolecular block copolymers led to the formation of large aggregates in aqueous solution with the increase in temperature. Notably, upon a further increase in temperature from 35 to 45 °C, the D_h values began to decrease from 300 to 190 nm, which might be attributed to the further dehydration of the PNIPAAM block at the higher temperature.[11b] Subsequently, VT DLS investigation of the aqueous solution of SBCP **5** after being treated with CO_2 was performed. The critical temperature was determined to be 35 °C, which is higher than that of the former aqueous solution of SBCP **5** without being treated with CO_2. This shift might be caused by the protonation of the amine groups of PDMAEMA though the addition of CO_2, making the block copolymer more water-soluble with the stronger hydrogen bonds between SBCP **5** and water molecules. Thus, in this case, it is necessary to increase the temperature to weaken the hydrogen bonds between the polymer and solvents, thus allowing for the aggregation of polymers in aqueous solution. As expected, after N_2 was passed through the solution to remove CO_2, the change tendency of the D_h returned to the initial state, and the growth trend of the curve was similar to that of the solution of SBCP **5** without being treated with CO_2. Variable-temperature (VT) ^{1}H NMR experiments in D_2O were further performed to investigate the CO_2-induced thermoresponsive behavior of SBCP **5**. Notably, the critical phase transition temperature obtained from ^{1}H NMR experiment (Figure S16) aligned with the DLS and UV results.

CO_2 Stimuli-Responsive Supramolecular Block Copolymer Hydrogels. In addition to the interesting CO_2-triggered morphology transformation and CO_2-induced thermoresponsive behavior of SBCP **5** in water, it is worth noting that SBCP **5** could form a supramolecular polymeric hydrogel cross-linked by well-defined metallacycles promoted by CO_2 near physiological temperature (34 °C). In a typical procedure of gelation, 30 mg of SBCP **5** was dissolved in 1.0 mL of water in a vial, followed by bubbling CO_2 for 1 min and subsequent heating to 34 °C. The free-standing macroscopic hydrogel was formed immediately (Figure 3). The critical gelation concentration (CGC) was determined to be 2.5 wt % for SBCP **5**. Notably, SBCP **5** was not able to form a free-standing gel at the same concentration without bubbling CO_2 (Figure S17e). Moreover, the gelation process was very fast, which could thus be considered as in situ generation of polymer hydrogels at 34 °C. When the temperature was cooled to room temperature, the hydrogel returned to a free-flowing, homogeneous solution. This recovered aqueous solution of

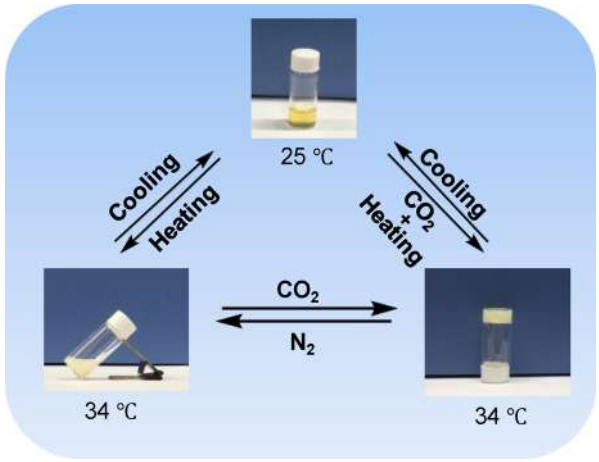

Figure 3. Reversible gel−sol transitions of supramolecular polymer gel **5** (3.0 wt %) triggered by CO_2/N_2 and temperature.

SBCP **5** reformed the hydrogel as the temperature increased to 34 °C. Interestingly, upon passing N_2 into the resultant supramolecular hydrogel of SBCP **5**, the gel-to-sol transition was observed within 2 min from top to bottom in the vial. The polymeric hydrogel **5** gradually collapsed and became a turbid solution, which ultimately became a transparent solution after cooling to room temperature (Figure 3). The hydrogel was reformed upon treatment of the resultant disassociated hydrogel with CO_2 for 1 min. Notably, this CO_2-switchable and thermo-reversible sol−gel transition could be repeatedly performed for several cycles.

To explore the key factors associated with the CO_2-promoted hydrogel formation, several control experiments were conducted (Scheme 3). First, the intermediate star

Scheme 3. Schematic Presentation of Several Model Polymers for the Gelation Test

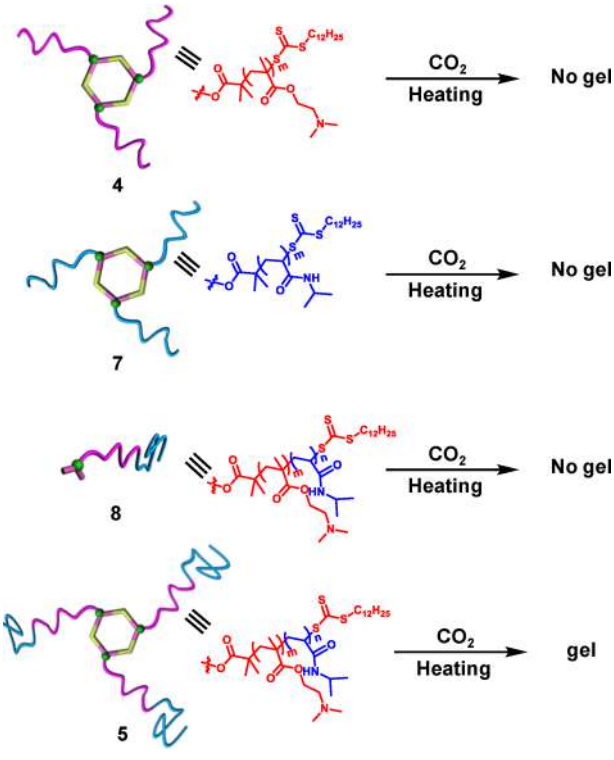

DOI: 10.1021/jacs.7b07303
J. Am. Chem. Soc. 2017, 139, 13811−13820

polymer **4** without PNIPAAM was investigated for hydrogel formation. Interestingly, at 34 °C, star polymer **4** was not able to form a free-standing gel at a similar concentration (3.0 wt %) after CO_2 bubbling (Figure S17a). In addition, the gel formation of another model star polymer **7**, containing three PNIPAAM arms rather than PDMAEMA, was studied at 34 °C after CO_2 inletting (Figure S17b), and no gel formation was found. To elucidate the influence of the metallacyclic scaffold on gelation, the linear copolymer PDMAEMA-*b*-PNIPAAM **8** without the metallacycle was designed and synthesized as another model polymer, and it was also unable to generate a hydrogel after inletting CO_2 at 34 °C (Figure S17c). Following the results of the control experiments, we assumed that the rigid metallacyclic core provided a well-defined, rigid scaffold, wherein the pendant polymer chains self-organized well to form the ordered nanostructures during the gelation process. Meanwhile, upon introducing CO_2 to the solution, the PDMAEMA block became protonated and more water-soluble, which made it easier to package water molecules. Upon increasing the temperature of the solution, the weakening hydrogen bonds between PNIPAAM chains and water induced a greater degree of block copolymer aggregation (Scheme 4). Thus, the coexistence of both block copolymers and the well-defined metallacycle is the key factor for the realization of CO_2-promoted hydrogel formation in this study.

Scheme 4. Schematic Presentation of the CO_2 Stimuli-Responsive Hydrogel of SBCP 5

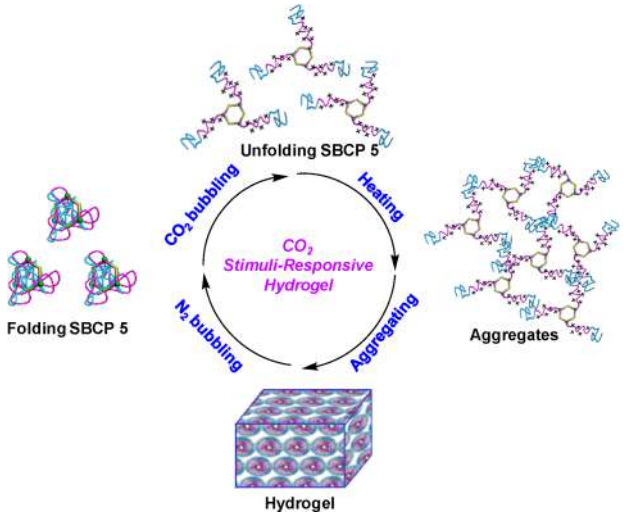

Rheological and viscosity investigations can provide further insight into the properties of cross-linked supramolecular materials.[18] Therefore, two rheological experiments were performed to examine the formation of supramolecular block copolymer hydrogels cross-linked by discrete metallacycles: (1) the linear response of the modulus (G' and G'') to a fixed small stress by varying the frequency and (2) nonlinear behavior of the modulus to a fixed frequency by varying the shear stress. As shown in Figure S18, for the hydrogel of SBCP **5**, a frequency sweep from 100 to 0.1 rad/s was performed at a small oscillatory stress of 1.0 Pa. It was found that the elastic modulus (G') of 100 Pa was higher than the viscous modulus (G''), with a linear response over the frequency range, which clearly identified the hydrogel-like behavior of SBCP **5**. Meanwhile, a strain sweep showed a linear region between 0.1% and 200% presenting a hydrogel-like behavior ($G' > G''$) and a liquid-like behavior ($G'' > G'$) above 200% (Figure S19). G' decreased rapidly above the yield stress, indicating the breakage of the networks.

It is well-known that the gel-phase transition can be determined from dynamic rheological data. To further study the CO_2-induced thermo-reversibility of the resultant hydrogel from SBCP **5**, dynamic shear moduli were tested on the prepared solutions after bubbling CO_2 within a temperature sweep range from 25 to 42 °C. As shown in Figure 4a, when

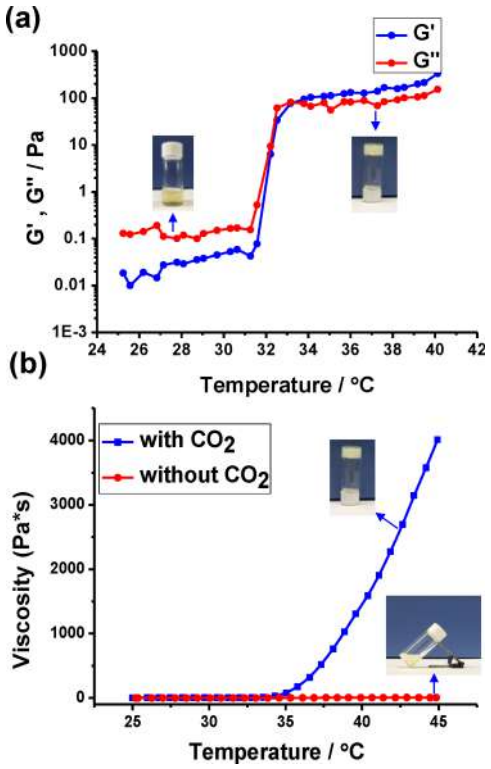

Figure 4. (a) Temperature dependence of dynamic shear moduli (σ = 1 Pa, ω = 1 rad/s) for a 3.0 wt % hydrogel of SBCP **5**. (b) Temperature dependence of the viscosity of SBCP **5** treated with CO_2 and without CO_2. Digital photos show the corresponding appearance.

the temperature was in the low region of 20 to 31.5 °C, both G' and G'' remained unchanged with the G'' always a little larger than G', confirming a liquid state. As the temperature was raised to 31.5 °C, both G' and G'' started to increase, and G' increased faster than G'', which was attributed to the sol−gel phase transition. The gelling point (T_{gel}) was determined to be 33 °C as indicated by the G'/G'' crossover point, which was related to the phase transition of the SBCP **5** hydrogel. The formation of the hydrogel was further investigated by viscosity-temperature oscillatory rheology for the aqueous solution of SBCP **5** (3.0 wt %). As shown in Figure 4b, no distinct change of the viscosity for the initial solution of SBCP **5** was observed between 25 and 45 °C. However, after bubbling CO_2, when the temperature reached 34 °C, the viscosity of **5** increased dramatically, suggesting the formation of a large three-dimensional (3D) network. Moreover, T_η was determined to be 34 °C according to the viscosity−temperature curves, which was close to the corresponding T_{gel}. To obtain further insight into the properties of the resultant block copolymer hydrogels, the effect of shear rates on the hydrogel viscosity was also

DOI: 10.1021/jacs.7b07303
J. Am. Chem. Soc. 2017, 139, 13811−13820

investigated. As shown in Figure S20, as the shear rate increased, the viscosity decreased, indicating a shear-thinning behavior due to the disruption of dynamic cross-links within the 3D networks of the gels.

Scanning electron microscopy (SEM) is a versatile technique that can elucidate the microscopic structure of supramolecular hydrogels. Thus, the morphology of the obtained xerogel from SBCP **5** was investigated by employing SEM, which revealed a 3D interconnected porous structure. As displayed in Figure 5a

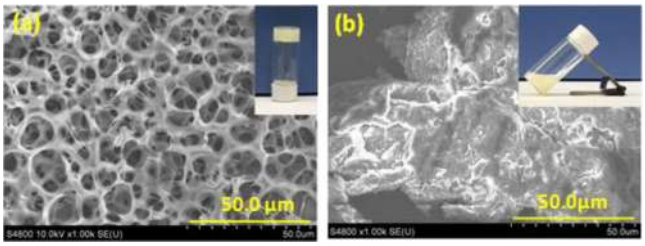

Figure 5. Photographs of polymeric hydrogel formation and SEM images of the xerogel: (a) SBCP **5** with CO_2 bubbling (b) SBCP **5** with N_2 bubbling.

and Figure S21, the average width of these pores was found to be approximately 10.0 μm. Notably, after N_2 bubbling, the regular porous networks were destroyed and turned into an irregular microstructure (Figure 5b and Figure S22). Moreover, to obtain further insight into the hydrogel formation process, the morphology of the cryo-dried solution of SBCP **5** at different temperatures after CO_2 bubbling (Figure S23) was also investigated. It was found that between 20 and 30 °C the SEM images exhibited disorderly fibers. However, when the temperature increased to 35 °C, uniform, highly ordered microstructures with a higher cross-link density were observed, demonstrating the formation of a supramolecular hydrogel. With the continuous increase in temperature, a decrease in pore size from approximately 20.0 to 8.0 μm with an enhanced cross-link density was found, which is consistent with the features of a typical cross-linked hydrogel.

Injectable and Biocompatible Hydrogel. Over the past two decades, injectable hydrogels have been extensively explored due to their wide biological applications including drug delivery, cell encapsulation, and tissue engineering.[19] Usually, injectable hydrogels are preferably designed in such a way that they are liquid-like during injection and form hydrogels only in situ in response to external stimuli such as pH, temperature, or ionic strength. The above-mentioned investigation revealed that SBCP **5** was able to form hydrogels near physiological temperature (34 °C) very quickly, thus prompting us to study the injectable property of the SBCP **5** hydrogel. As described below, first, SBCP **5** was dissolved in water at room temperature with a fixed concentration (3.0 wt %). Then, sulforhodamine B (a fluorescent dye) was added into the aqueous solution of SBCP **5**, which was then stirred for a few minutes. After ventilation with CO_2 for 1 min, the solution was pipetted into a syringe. Upon injection into the aqueous media at 34 °C, the SBCP **5** hydrogel formed immediately. The whole process was recorded by camera. Upon increasing time, the volume of the hydrogel in the water gradually increased (Figure 6 and movie 1).

Inspired by CO_2 stimuli-responsive gel-to-sol transition and good injection profile, we envisioned that obtained supramolecular hydrogels cross-linked by discrete metallacycles might be very promising to be explored as biological materials. Thus, the cytotoxicity of SBCP **5** was first investigated by conducting a MTT assay of the MC-3T3 cell line after 24 h incubation. Figure 7a shows the influence of polymer concentration (0.05−0.5 mg/mL in media) on MC-3T3 cell viability. It was found that the SBCP **5** exhibited a dose-dependent cytotoxicity effect. When the polymer concentration of SBCP **5** was up to 0.5 mg/mL, the cell viability was found to be above 80%, indicating the low cytotoxicity of the obtained block copolymer.

Moreover, to investigate the biocompatibility of the resultant hydrogel from SBCP **5**, cell culture studies were further employed to evaluate its in vitro cytotoxicity. MC-3T3 cells were encapsulated in the hydrogels of SBCP **5**. After being incubated with 50 or 125 μL of hydrogel SBCP **5** (3.0 wt %) for 24 h, the MC-3T3 cells were stained by using a Live/Dead assay kit. Then fluorescence micrographs were obtained under an inverted microscope to distinguish the living cells (green fluorescence) from the dead (red fluorescence). As shown in Figure 7c, when MC-3T3 cells were incubated with 50 μL of the SBCP **5** hydrogel for 24 h, over 95% living cells were observed, and red fluorescence could hardly be observed in the micrographs. Even after being incubated with 125 μL of SBCP **5** hydrogel for 24 h, 90% living cells were observed compared with those of the control group (Figure 7d). These obtained results suggested that the resultant SBCP hydrogel featured good cytocompatibility.

■ CONCLUSION

In summary, by combining coordination-driven self-assembly and *stepwise* postpolymerization, we successfully realized the construction of a new family of supramolecular star block copolymers (SBCPs) containing discrete, well-defined metallacycles as cores. Notably, from the resultant SBCP, supramolecular polymeric hydrogels cross-linked by discrete metal-

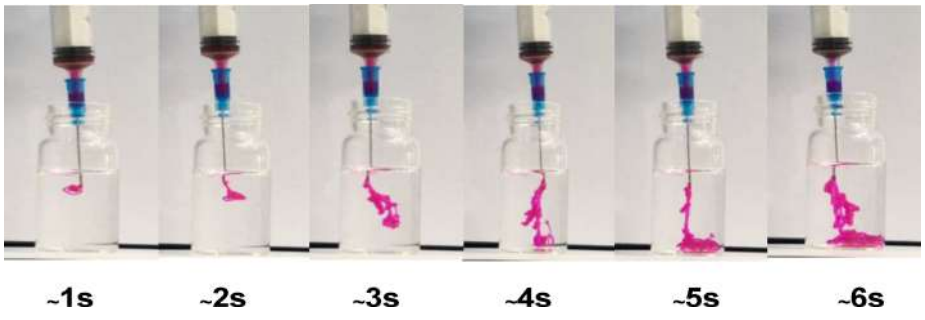

Figure 6. Photographs of the injectable hydrogel over time at 34 °C.

DOI: 10.1021/jacs.7b07303
J. Am. Chem. Soc. 2017, 139, 13811−13820

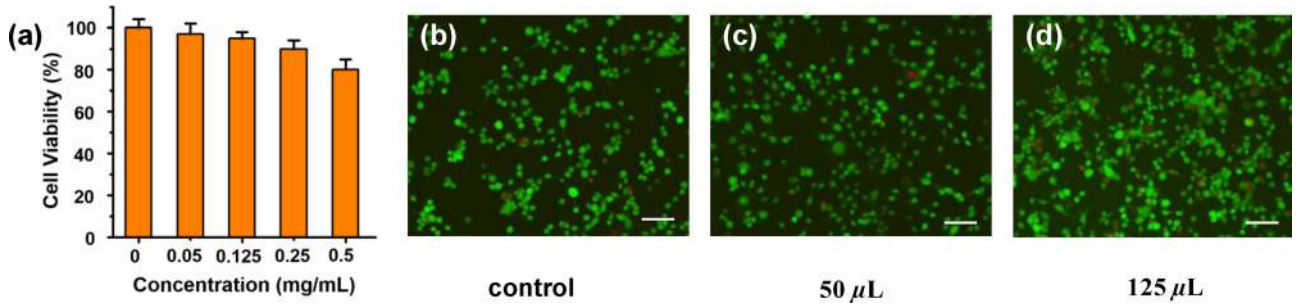

Figure 7. Cell viability of MC-3T3 treated with different concentrations of SBCP **5** (a). Fluorescent microscopy images of MC-3T3 in the SBCP **5** hydrogel after 24 h incubation with 0 (b), 50 (c), and 125 μL (d) (scale bar = 100 μm).

lacycles were obtained, promoted by CO_2 near physiological temperature, which is unlike most known supramolecular polymer gels cross-linked by discrete organometallic architectures that are usually generated in organic solvents. Moreover, a series of control experiments disclosed that the coexistence of both block copolymers and well-defined metallacycles was the key factor for the realization of CO_2-promoted hydrogel formation in this study. Further investigation revealed that these obtained hydrogels featured CO_2-switchable, injectable, and cytocompatible properties. To the best of our knowledge, this study provides the first example of CO_2-switchable block copolymer hydrogels cross-linked by well-defined, discrete MOMs, which were injectable and had good cytocompatibility, thus providing a new route for the preparation of novel "smart" soft matter with potential as biological materials.

■ EXPERIMENTAL SECTION

Full experimental details are provided in the Supporting Information. The most important information is summarized below.

General Information. All reagents were commercially available and used as received unless stated otherwise. *N*-Isopropylacrylamide (NIPAAM, recrystallized twice from hexane prior to use) and azodiisobutyronitrile (AIBN, recrystallized from ethanol before use) were purchased from Energy Chemical Reagent Co. J & K. TLC analyses were performed on silica gel plates, and flash chromatography was conducted using silica gel column packages. All solvents were dried according to standard procedures, and all of them were degassed under N_2 for 30 min before use. All air-sensitive reactions were performed under argon atmosphere. ^{1}H NMR and ^{31}P NMR spectra were recorded on a Bruker 400 MHz spectrometer (^{1}H: 400 MHz; ^{31}P: 161.9 MHz) and a Bruker 500 MHz spectrometer (^{1}H: 500 MHz) at 298 K. The ^{1}H chemical shifts are reported relative to residual solvent signals, and ^{31}P NMR resonances are referenced to an internal standard sample of 85% H_3PO_4 (δ 0.0). Coupling constants (J) are denoted in Hz and chemical shifts (δ) in ppm. Multiplicities are denoted as follows: s = singlet, d = doublet, m = multiplet, br = broad. IR spectra were recorded on a Bruker Tensor 27 infrared spectrophotometer. Tris-CTA metallacycle **3** was prepared through the previous procedure in literature.[2c]

Transmission Electron Microscopy and Dynamic Light Scattering Studies. TEM images were recorded on a Tecnai G^2 F30 (FEI Ltd.). The samples for TEM measurement were prepared by dropping the solution onto a carbon-coated copper grid. Dynamic light scattering was recorded by a Zetasizer Nano ZS90 from Malvern Instruments (UK).

Scanning Electron Microscopy and Confocal Laser Scanning Microscopy. The SEM samples were prepared on clean Si substrates. To minimize sample charging, a thin layer of Au was deposited onto the samples before examination. All the SEM images were obtained using an S-4800 (Hitachi Ltd.) with an accelerating voltage of 3.0–10.0 kV. Confocal laser scanning microscopy (CLSM) imaging was performed with an OLYMPUS ZX81 laser scanning microscope and a 60× oil-immersion objective lens.

Gel Permeation Chromatography (GPC) Protocols. A gel permeation chromatograph equipped with a Waters 1515 isocratic HPLC pump and a Waters 2414 refractive index detector was used to perform GPC measurements at 40 °C using THF containing 5 mM LiTFSI, 5 mM 1-butylimidazole, and 0.02 wt % BHT as eluent with a flow rate of 1.0 mL/min. The system was calibrated with polystyrene standards. THF and sample solutions were filtered over a filter with a pore size of 0.22 μm (PTFE, Millex-HN 13 mm Syringes Filters, Millipore, US).

Dynamic Rheology Measurements. Rheological measurements were performed on freshly prepared gels using a controlled stress rheometer (HAAKE MARSIII, Thermo Fisher). A parallel plate geometry with a 25 mm diameter and a 0.3 mm gap was employed throughout dynamic oscillatory work.

Cytotoxicity of SBCP 5. It is well-known that MC-3T3, which is an osteoblast precursor cell line derived from *Mus musculus* (mouse) calvaria, features the stronger sensitivity to the input stimulus when compared to L929 and some completely differentiated cells. Thus, MC-3T3 was chosen for the biocompatibility investigation of SBCP **5**. They were obtained from Institute of Biochemistry and Cell Biology, Chinese Academy of Sciences, Shanghai, China. The cells were cultured with DMEM (10% fetal bovine serum, 5% CO_2 at 37 °C). MC-3T3 cells, specifically, 5×10^3 cells in each well were seeded in 96-well plates and incubated for 24 h. Then, each cell was exposed to a different concentration of SBCP **5** samples and incubated for another 24 h. Next, 20 μL MTT solutions were added to each well, and cells were incubated for 4 h. After removing all of the solution in each well, 150 μL of DMSO (per well) was added before measurement at 490 nm; cells cultured without SBCP **5** were explored as a control.

Live/Dead Staining Analysis. MC-3T3 (1.8×10^5 cells, 1.0 mL DMEM medium for each well) were seeded in 3422 transwell plate and incubated with 50 or 125 μL of hydrogel SBCP **5** (3.0 wt %) for 24 h. Then the live cells were stained with Calcein-AM (green), and dead cells were stained with propidium iodide (red). Each sample was set in triplicate.

Synthesis of Intermediate Star Supramolecular Polymer 4. Supramolecular tris-CTA hexagon **3** (47 mg, 7.90 μmol), AIBN (0.65 mg, 3.95 μmol), *N*,*N*-dimethylaminoethyl methacrylate (745 mg, 4.7 mmol), and 1.5 mL of acetone were added into a 10.0 mL flask equipped with a magnetic stir bar. After being degassed by three freeze–pump–thaw cycles, the mixed solution was immediately transferred to a preheated oil bath at 60 °C to initiate the polymerization. After 20 h, the polymerization was quenched by liquid N_2, and the resultant mixture was precipitated in cold *n*-hexane. The precipitate was dissolved in acetone and then precipitated again in the presence of *n*-hexane. The above dissolution–precipitation cycle was repeated three times. The final product was dried in vacuum, yielding a yellow solid: 425 mg, $M_{n,\,NMR}$ = 55.4 kDa, $M_{n,\,GPC}$ = 42.1 kDa, PDI = 1.23; ^{1}H NMR (acetone-d_6, 400 MHz) 4.07 (s, -O–CH_2-), 2.58 (s, CH_3 end-group), 0.95–0.96 (s, –CH_3); ^{31}P NMR (acetone-d_6, 161.9 MHz) δ 14.43 (s, J_{Pt-P} = 2726 Hz); IR (neat) 3396, 2940, 2932, 2821, 2770, 1721, 1575, 1146, 1058 cm^{-1}.

DOI: 10.1021/jacs.7b07303
J. Am. Chem. Soc. 2017, 139, 13811–13820

Synthesis of SBCP 5. Supramolecular star polymer **4** (425 mg), AIBN (0.65 mg, 3.95 μmol), *N*-isopropylacryamide (536 mg, 4.7 mmol), and 1.5 mL of acetone were added into a 10.0 mL flask equipped with a magnetic stir bar. After being degassed by three freeze−pump−thaw cycles, the mixed solution was immediately transferred to a preheated oil bath at 60 °C to initiate the polymerization. After 20 h, the polymerization was quenched by liquid N_2, and the resultant mixture was precipitated in diethyl ether. The precipitate was dissolved in acetone and then precipitated again in the presence of diethyl ether. The above dissolution−precipitation cycle was repeated three times. The final product was dried in vacuum, yielding a yellow solid: 480 mg, $M_{n,NMR}$ = 96.5 kDa, $M_{n,GPC}$ = 76.3 kDa, PDI = 1.30; ^{1}H NMR (acetone-d_6, 400 MHz): 6.80−7.45 (br s, −N*H*), 4.00 (br s, NC*H*), 1.1−2.06 (br m, backbone),0.84−0.88 (s, CH_3 end-group); ^{31}P NMR (acetone-d_6, 161.9 MHz) δ 14.41 (s, J_{Pt-P} = 2716 Hz); IR (neat) 3468, 3291, 3072, 2971, 2936, 1727, 1639, 1544, 1271, 1239 cm^{-1}.

■ ASSOCIATED CONTENT

Supporting Information

The Supporting Information is available free of charge on the ACS Publications website at DOI: 10.1021/jacs.7b07303.

Synthesis, characterization, and other experimental details (PDF)

Movie showing the injection of the hydrogel (AVI)

■ AUTHOR INFORMATION

Corresponding Authors

*hbyang@chem.ecnu.edu.cn

*guosong@fudan.edu.cn

ORCID

Guosong Chen: 0000-0001-7089-911X

Hai-Bo Yang: 0000-0003-4926-1618

Notes

The authors declare no competing financial interest.

■ ACKNOWLEDGMENTS

H.-B.Y acknowledges the financial support of the 973 Program (No. 2015CB856600), NSFC/China (No. 21625202), STCSM (No. 16XD1401000), and the Program for Changjiang Scholars and Innovative Research Team in University. G.C. acknowledges the support of NSFC/China (Nos. 91527305, 21474020, 91227203, and 51322306).

■ REFERENCES

(1) (a) Terech, P.; Weiss, R. G. *Chem. Rev.* **1997**, *97*, 3133. (b) Sangeetha, N. M.; Maitra, U. *Chem. Soc. Rev.* **2005**, *34*, 821. (c) Yang, Z.; Liang, G.; Xu, B. *Acc. Chem. Res.* **2008**, *41*, 315. (d) Hirst, A. R.; Escuder, B.; Miravet, J. F.; Smith, D. K. *Angew. Chem., Int. Ed.* **2008**, *47*, 8002. (e) Foster, J. A.; Piepenbrock, M.-O. M.; Lloyd, G. O.; Clarke, N.; Howard, J. A. K.; Steed, J. W. *Nat. Chem.* **2010**, *2*, 1037. (f) Piepenbrock, M.-O. M.; Lloyd, G. O.; Clarke, N.; Steed, J. W. *Chem. Rev.* **2010**, *110*, 1960. (g) Appel, E. A.; del Barrio, J.; Loh, X. J.; Scherman, O. A. *Chem. Soc. Rev.* **2012**, *41*, 6195. (h) Yan, X.; Wang, F.; Zheng, B.; Huang, F. *Chem. Soc. Rev.* **2012**, *41*, 6042. (i) Li, Y.; Rodrigues, J.; Tomas, H. *Chem. Soc. Rev.* **2012**, *41*, 2193. (j) Du, X.; Zhou, J.; Shi, J.; Xu, B. *Chem. Rev.* **2015**, *115*, 13165. (k) Ma, X.; Zhao, Y. *Chem. Rev.* **2015**, *115*, 7794. (l) Liu, M.; Zhang, L.; Wang, T. *Chem. Rev.* **2015**, *115*, 7304. (m) Bhattacharya, S.; Samanta, S. K. *Chem. Rev.* **2016**, *116*, 11967.

(2) (a) Yan, X.; Li, S.; Pollock, J. B.; Cook, T. R.; Chen, J.; Zhang, Y.; Ji, X.; Yu, Y.; Huang, F.; Stang, P. J. *Proc. Natl. Acad. Sci. U. S. A.* **2013**, *110*, 15585. (b) Li, Z.-Y.; Zhang, Y.-Y.; Zhang, C.-W.; Chen, L.-J.; Wang, C.; Tan, H.; Yu, Y.; Li, X.; Yang, H.-B. *J. Am. Chem. Soc.* **2014**, *136*, 8577. (c) Zheng, W.; Chen, L.-J.; Yang, G.; Sun, B.; Wang, X.; Jiang, B.; Yin, G.-Q.; Zhang, L.; Li, X.; Liu, M.; Chen, G.; Yang, H.-B. *J. Am. Chem. Soc.* **2016**, *138*, 4927. (d) Yan, X.; Li, S.; Cook, T. R.; Ji, X.; Yao, Y.; Pollock, J. B.; Shi, Y.; Yu, G.; Li, j.; Huang, F.; Stang, P. J. *J. Am. Chem. Soc.* **2013**, *135*, 14036.

(3) (a) Zhukhovitskiy, A. V.; Zhong, M.; Keeler, E. G.; Michaelis, V. K.; Sun, J. E. P.; Hore, M. J. A.; Pochan, D. J.; Griffin, R. G.; Willard, A. P.; Johnson, J. A. *Nat. Chem.* **2016**, *8*, 33. (b) Wang, Y.; Zhong, M.; Park, J. V.; Zhukhovitskiy, A. V.; Shi, W.; Johnson, J. A. *J. Am. Chem. Soc.* **2016**, *138*, 10708. (c) Kawamoto, K.; Grindy, S. C.; Liu, J.; Holten-Andersen, N.; Johnson, J. *ACS Macro Lett.* **2015**, *4*, 458. (d) Foster, J. A.; Parker, R. M.; Belenguer, A. M.; Kishi, N.; Sutton, S.; Abell, C.; Nitschke, J. R. *J. Am. Chem. Soc.* **2015**, *137*, 9722. (e) Wang, Y.; Gu, Y.; Keeler, E. G.; Park, J. V.; Griffin, R. G.; Johnson, J. A. *Angew. Chem., Int. Ed.* **2017**, *56*, 188.

(4) (a) Wang, Z.; Cohen, S. M. *Chem. Soc. Rev.* **2009**, *38*, 1315. (b) Deng, H.; Doonan, C. J.; Furukawa, H.; Ferreira, R. B.; Towne, J.; Knobler, C. B.; Wang, B.; Yaghi, O. M. *Science* **2010**, *327*, 846. (c) Tanabe, K. K.; Cohen, S. M. *Chem. Soc. Rev.* **2011**, *40*, 498. (d) Chakrabarty, R.; Stang, P. J. *J. Am. Chem. Soc.* **2012**, *134*, 14738. (e) Chen, S.; Chen, L.-J.; Yang, H.-B.; Tian, H.; Zhu, W. *J. Am. Chem. Soc.* **2012**, *134*, 13596. (f) Roberts, D. A.; Pilgrim, B. S.; Cooper, J. D.; Ronson, T. K.; Zarra, S.; Nitschke, J. R. *J. Am. Chem. Soc.* **2015**, *137*, 10068. (g) Ronson, T. K.; Pilgrim, B. S.; Nitschke, J. R. *J. Am. Chem. Soc.* **2016**, *138*, 10417.

(5) (a) Stang, P. J.; Olenyuk, B. *Acc. Chem. Res.* **1997**, *30*, 502. (b) Fujita, M.; Tominaga, M.; Hori, A.; Therrien, B. *Acc. Chem. Res.* **2005**, *38*, 369. (c) Pluth, M. D.; Raymond, K. N. *Chem. Soc. Rev.* **2007**, *36*, 161. (d) Liu, S.; Han, Y.-F.; Jin, G.-X. *Chem. Soc. Rev.* **2007**, *36*, 1543. (e) Oliveri, C. G.; Ulmann, P. A.; Wiester, M. J.; Mirkin, C. A. *Acc. Chem. Res.* **2008**, *41*, 1618. (f) Chakrabarty, R.; Mukherjee, P. S.; Stang, P. J. *Chem. Rev.* **2011**, *111*, 6810. (g) Takezawa, Y.; Shionoya, M. *Acc. Chem. Res.* **2012**, *45*, 2066. (h) Castilla, A.; Ramsay, W.; Nitschke, J. R. *Acc. Chem. Res.* **2014**, *47*, 2063. (i) Han, M.; Engelhard, D. M.; Clever, G. H. *Chem. Soc. Rev.* **2014**, *43*, 1848. (j) Han, Y.-F.; Jin, G.-X. *Acc. Chem. Res.* **2014**, *47*, 3571. (k) Yoshizawa, M.; Klosterman, J. K. *Chem. Soc. Rev.* **2014**, *43*, 1885. (l) Cook, T. R.; Stang, P. J. *Chem. Rev.* **2015**, *115*, 7001. (m) McConnell, A. J.; Wood, C. S.; Neelakandan, P. P.; Nitschke, J. R. *Chem. Rev.* **2015**, *115*, 7729. (n) Xu, L.; Wang, Y.-X.; Chen, L.-J.; Yang, H.-B. *Chem. Soc. Rev.* **2015**, *44*, 2148. (o) Wang, W.; Wang, Y.-X.; Yang, H.-B. *Chem. Soc. Rev.* **2016**, *45*, 2656. (p) Chen, L.-J.; Yang, H.-B.; Shionoya, M. *Chem. Soc. Rev.* **2017**, *46*, 2555. (q) Cook, T. R.; Vajpayee, V.; Lee, M. H.; Stang, P. J.; Chi, K. *Acc. Chem. Res.* **2013**, *46*, 2464.

(6) (a) Fujita, M.; Yazaki, J.; Ogura, K. *J. Am. Chem. Soc.* **1990**, *112*, 5645. (b) Stang, P. J.; Cao, D. H. *J. Am. Chem. Soc.* **1994**, *116*, 4981. (c) Fujita, M.; Oguro, D.; Miyazawa, M.; Oka, H.; Yamaguchi, K.; Ogura, K. *Nature* **1995**, *378*, 469. (d) Stang, P. J.; Olenyuk, B.; Whiteford, J. A.; Fechtenkotter, A. *Nature* **1999**, *398*, 796. (e) Brown, A. M.; Ovchinnikov, M. V.; Stern, C. L.; Mirkin, C. A. *J. Am. Chem. Soc.* **2004**, *126*, 14316. (f) Wang, P.; Moorefield, C. N.; Newkome, G. R. *Angew. Chem., Int. Ed.* **2005**, *44*, 1679. (g) Dong, V. M.; Fiedler, D.; Carl, B.; Bergman, R. G.; Raymond, K. N. *J. Am. Chem. Soc.* **2006**, *128*, 14464. (h) Harano, K.; Hiraoka, S.; Shionoya, M. *J. Am. Chem. Soc.* **2007**, *129*, 5300. (i) Hiraoka, S.; Harano, K.; Shiro, M.; Shionoya, M. *J. Am. Chem. Soc.* **2008**, *130*, 14368. (j) Kishi, N.; Li, Z.; Yoza, K.; Akita, M.; Yoshizawa, M. *J. Am. Chem. Soc.* **2011**, *133*, 11438. (k) Meng, W.; Clegg, J. K.; Thoburn, J. D.; Nitschke, J. R. *J. Am. Chem. Soc.* **2011**, *133*, 13652. (l) Clever, G. H.; Kawamura, W.; Tashiro, S.; Shiro, M.; Shionoya, M. *Angew. Chem., Int. Ed.* **2012**, *51*, 2606. (m) Yan, X.; Jiang, B.; Cook, T. R.; Zhang, Y.; Li, J.; Yu, Y.; Huang, F.; Yang, H.-B.; Stang, P. J. *J. Am. Chem. Soc.* **2013**, *135*, 16813. (n) Freye, S.; Michel, R.; Stalke, D.; Pawliczek, M.; Frauendorf, H.; Clever, G. H. *J. Am. Chem. Soc.* **2013**, *135*, 8476. (o) Kishi, N.; Akita, M.; Kamiya, M.; Hayashi, S.; Hsu, H.-F.; Yoshizawa, M. *J. Am. Chem. Soc.* **2013**, *135*, 12976. (p) Wood, C. S.; Ronson, T. K.; Belenguer, A. M.; Holstein, J. J.; Nitschke, J. R. *Nat. Chem.* **2015**, *7*, 354. (q) Roy, B.; Ghosh, A. K.; Srivastava, S.; Mukherjee, P. S. *J. Am. Chem. Soc.* **2015**, *137*, 11916. (r) Bhat, I. A.; Samanta, D.; Mukherjee, P. S. *J. Am. Chem. Soc.* **2015**, *137*, 9497. (s) Zhu, R.; Lübben, J.; Dittrich, B.; Clever, G.

H. *Angew. Chem., Int. Ed.* **2015**, *54*, 2796. (t) Mondal, B.; Acharyya, K.; Howlader, P.; Mukherjee, P. S. *J. Am. Chem. Soc.* **2016**, *138*, 1709. (u) Jiang, B.; Zhang, J.; Ma, J.-Q.; Zheng, W.; Chen, L.-J.; Sun, B.; Li, C.; Hu, B.-W.; Tan, H.; Li, X.; Yang, H.-B. *J. Am. Chem. Soc.* **2016**, *138*, 738. (v) Chen, L.-J.; Jiang, B.; Yang, H.-B. *Org. Chem. Front.* **2016**, *3*, 579. (w) Jiang, B.; Chen, L.-J.; Zhang, Y.; Tan, H.-W.; Xu, L.; Yang, H.-B. *Chin. Chem. Lett.* **2016**, *27*, 607. (x) Fujita, D.; Ueda, Y.; Sato, S.; Yokoyama, H.; Mizuno, N.; Kumasaka, T.; Fujita, M. *Chem.* **2016**, *1*, 91−101. (y) Samanta, S. K.; Moncelet, D.; Briken, V.; Isaacs, L. *J. Am. Chem. Soc.* **2016**, *138*, 14488. (z) Oldacre, A. N.; Friedman, A. E.; Cook, T. R. *J. Am. Chem. Soc.* **2017**, *139*, 1424.

(7) (a) Yan, Q.; Zhao, Y. *Chem. Commun.* **2014**, *50*, 11631. (b) Darabi, A.; Jessop, P. G.; Cunningham, M. F. *Chem. Soc. Rev.* **2016**, *45*, 4391. (c) Girard, E.; Tassaing, T.; Marty, J.-D.; Destarac, M. *Chem. Rev.* **2016**, *116*, 4125.

(8) (a) Ochiai, B.; Yokota, K.; Fujii, A.; Nagai, D.; Endo, T. *Macromolecules* **2008**, *41*, 1229. (b) Yan, Q.; Yin, Y.; Yuan, J. *Angew. Chem., Int. Ed.* **2011**, *50*, 4923. (c) Lu, W.; Sculley, J. P.; Yuan, D.; Krishna, R.; Wei, Z.; Zhou, H. C. *Angew. Chem., Int. Ed.* **2012**, *51*, 7480. (d) Yan, Q.; Zhao, Y. *J. Am. Chem. Soc.* **2013**, *135*, 16300. (e) Ma, Y.; Yung, L. Y. L. *Anal. Chem.* **2014**, *86*, 2429. (f) Yu, G.; Lu, Y.; Liu, X.; Wang, W.-J.; Yang, Q.; Xing, H.; Ren, Q.; Li, B.-G.; Zhu, S. *Ind. Eng. Chem. Res.* **2014**, *53*, 16025.

(9) (a) Gutknecht, J.; Bisson, M. A.; Tosteson, F. C. *J. Gen. Physiol.* **1977**, *69*, 779. (b) Kim, S.-H.; Kelly, P. B.; Clifford, A. J. *Anal. Chem.* **2008**, *80*, 7651. (c) Liu, Z.; Hu, Y.; Zhao, H.; Wang, Y.; Xu, H.; Pan, H.; Tang, R. *Phys. Chem. Chem. Phys.* **2015**, *17*, 10080.

(10) (a) Nagai, D.; Suzuki, A.; Kuribayashi, T. *Macromol. Rapid Commun.* **2011**, *32*, 404. (b) Han, D.; Boissiere, O.; Kumar, S.; Tong, X.; Tremblay, L.; Zhao, Y. *Macromolecules* **2012**, *45*, 7440. (c) Hoshino, Y.; Imamura, K.; Yue, M.; Inoue, G.; Miura, Y. *J. Am. Chem. Soc.* **2012**, *134*, 18177. (d) Morse, A. J.; Armes, S. P.; Thompson, K. L.; Dupin, D.; Fielding, L. A.; mills, P.; Swart, R. *Langmuir* **2013**, *29*, 5466.

(11) (a) Schild, H. G.; Tirrell, D. A. *Macromolecules* **1992**, *25*, 4553. (b) Qiu, X.; Kwan, S.; Wu, C. *Macromolecules* **1997**, *30*, 6090. (c) Liu, J.; Chen, G.; Guo, M.; Jiang, M. *Macromolecules* **2010**, *43*, 8086. (d) Jochum, F. D.; Theato, P. *Chem. Soc. Rev.* **2013**, *42*, 7468. (e) Roy, D.; Brooks, W. L. A.; Sumerlin, B. S. *Chem. Soc. Rev.* **2013**, *42*, 7214. (f) Seeboth, A.; Lotzsch, D.; Ruhmann, R.; Muehling, O. *Chem. Rev.* **2014**, *114*, 3037.

(12) (a) Yan, B.; Han, D.; Boissiere, O.; Ayotte, P.; Zhao, Y. *Soft Matter* **2013**, *9*, 2011. (b) Liu, B.; Zhou, H.; Zhou, S.; Zhang, H.; Feng, A.; Jian, C.; Hu, J.; Gao, W.; Yuan, J. *Macromolecules* **2014**, *47*, 2938. (c) Du, J. Z.; Armes, S. P. *J. Am. Chem. Soc.* **2005**, *127*, 12800.

(13) (a) Zhao, G.-Z.; Li, Q.-J.; Chen, L.-J.; Tan, H.; Wang, C.-H.; Wang, D.-X.; Yang, H.-B. *Organometallics* **2011**, *30*, 5141. (b) Chen, L.-J.; Li, Q.-J.; He, J.; Tan, H.; Abliz, Z.; Yang, H.-B. *J. Org. Chem.* **2012**, *77*, 1148. (c) Wu, N.-W.; Zhang, J.; Ciren, D.; Han, Q.; Chen, L.-J.; Xu, L.; Yang, H.-B. *Organometallics* **2013**, *32*, 2536. (d) Wang, W.; Zhang, Y.; Sun, B.; Chen, L.-J.; Xu, X.-D.; Wang, M.; Li, X.; Yu, Y.; Jiang, W.; Yang, H.-B. *Chem. Sci.* **2014**, *5*, 4554. (e) Wang, W.; Sun, B.; Wang, X.-Q.; Ren, Y.-Y.; Chen, L.-J.; Ma, J.; Zhang, Y.; Li, X.; Yu, Y.; Tan, H.; Yang, H.-B. *Chem. - Eur. J.* **2015**, *21*, 6286. (f) Sun, B.; Wang, M.; Lou, Z.; Huang, M.; Xu, C.; Li, X.; Chen, L.-J.; Yu, Y.; Davis, G. L.; Xu, B.; Yang, H.-B.; Li, X. *J. Am. Chem. Soc.* **2015**, *137*, 1556. (g) Chen, L.-J.; Ren, Y.-Y.; Wu, N.-W.; Sun, B.; Ma, J.-Q.; Tan, H.; Liu, M.; Li, X.; Yang, H.-B. *J. Am. Chem. Soc.* **2015**, *137*, 11725. (h) Chen, L.-J.; Ren, Y.-Y.; Wu, N.-W.; Sun, B.; Ma, J.-Q.; Tan, H.; Liu, M.; Li, X.; Yang, H.-B. *J. Am. Chem. Soc.* **2015**, *137*, 11725. (i) Zheng, W.; Yang, G.; Jiang, S.-T.; Shao, N.; Yin, G.-Q.; Xu, L.; Li, X.; Chen, G.; Yang, H.-B. *Mater. Chem. Front.* **2017**, *1*, 1823. (j) Huang, C.-B.; Xu, L.; Zhu, J.-L.; Wang, Y.-X.; Sun, B.; Li, X.; Yang, H.-B. *J. Am. Chem. Soc.* **2017**, *139*, 9459.

(14) (a) Braunecker, W.; Matyjaszewski, K. *Prog. Polym. Sci.* **2007**, *32*, 93. (b) Zetterlund, P. B.; Kagawa, Y. *Chem. Rev.* **2008**, *108*, 3747. (c) Yamago, S. *Chem. Rev.* **2009**, *109*, 5051. (d) Rosen, B. M.; Percec, V. *Chem. Rev.* **2009**, *109*, 5069. (e) Chen, M.; Zhong, M.; Johnson, J. A. *Chem. Rev.* **2016**, *116*, 10167.

(15) (a) Newkome, G. R.; Yao, Z.; Baker, G. R.; Gupta, V. K. *J. Org. Chem.* **1985**, *50*, 2003. (b) Hosono, N.; Gillissen, M. A. J.; Li, Y.; Sheiko, S. S.; Palmans, A. R. A.; Meijer, E. W. *J. Am. Chem. Soc.* **2013**, *135*, 501. (c) Porsch, C.; Zhang, Y.; Ducani, C.; Vilaplana, F.; Nordstierna, L.; Nyström, A. M.; Malmström, E. *Biomacromolecules* **2014**, *15*, 2235. (d) Porsch, C.; Zhang, Y.; Montanez, M. I.; Malho, J.-M.; Kostiainen, M. A.; Nyström, A. M.; Malmström, E. *Biomacromolecules* **2015**, *16*, 2872. Xing, H.; Bai, Y.; Bai, Y.; Tan, L. H.; Tao, J.; Pedretti, B.; Vincil, G. A.; Lu, Y.; Zimmerman, S. C. *J. Am. Chem. Soc.* **2017**, *139*, 3623.

(16) (a) Liu, K.; Wang, C.; Li, Z.; Zhang, X. *Angew. Chem., Int. Ed.* **2011**, *50*, 4952. (b) Wang, C.; Wang, Z.; Zhang, X. *Acc. Chem. Res.* **2012**, *45*, 608. (c) Tao, W.; Liu, Y.; Jiang, B.; Yu, S.; Huang, W.; Zhou, Y.; Yan, D. *J. Am. Chem. Soc.* **2012**, *134*, 762. (d) Jie, K.; Zhou, Y.; Yao, Y.; Shi, B.; Huang, F. *J. Am. Chem. Soc.* **2015**, *137*, 10472. (e) Chi, X.; Ji, X.; Xia, D.; Huang, F. *J. Am. Chem. Soc.* **2015**, *137*, 1440. (f) Wang, Y.-X.; Zhang, Y.-M.; Liu, Y. *J. Am. Chem. Soc.* **2015**, *137*, 4543. (g) Chi, X.; Yu, G.; Shao, L.; Chen, J.; Huang, F. *J. Am. Chem. Soc.* **2016**, *138*, 3168.

(17) (a) Wu, C.; Zhou, S. *Macromolecules* **1995**, *28*, 8381. (b) Sundararaman, A.; Stephan, T.; Grubbs, R. B. *J. Am. Chem. Soc.* **2008**, *130*, 12264. (c) Moughton, A. O.; O'reilly, R. K. *Chem. Commun.* **2010**, *46*, 1091. (d) Cai, Y.; Aubrecht, K. B.; Grubbs, R. B. *J. Am. Chem. Soc.* **2011**, *133*, 1058.

(18) (a) Yount, W. C.; Loveless, D. M.; Craig, S. L. *Angew. Chem., Int. Ed.* **2005**, *44*, 2746. (b) Xu, D.; Hawk, J.; Loveless, D. M.; Jeon, S. L.; Craig, S. L. *Macromolecules* **2010**, *43*, 3556. (c) Xu, D.; Liu, C. Y.; Craig, S. L. *Macromolecules* **2011**, *44*, 2343. (d) Xu, D.; Craig, S. L. *Macromolecules* **2011**, *44*, 5465.

(19) (a) Kretlow, J. D.; Klouda, L.; Mikos, A. G. *Adv. Drug Delivery Rev.* **2007**, *59*, 263. (b) Kope cek, J. *Biomaterials* **2007**, *28*, 5185. (c) Yu, L.; Ding, J. *Chem. Soc. Rev.* **2008**, *37*, 1473. (d) Joo, M. K.; Park, M. H.; Choi, B. G.; Jeong, B. *J. Mater. Chem.* **2009**, *19*, 5891. (e) Sivakumaran, D.; Maitland, D.; Hoare, T. *Biomacromolecules* **2011**, *12*, 4112.

DOI: 10.1021/jacs.7b07303
J. Am. Chem. Soc. 2017, 139, 13811−13820